CHAOTIC AND BIFURCATION BEHAVIOR IN AN AUTONOMOUS FLIP-FLOP CIRCUIT USED BY PIECEWISE LINEAR TUNNEL DIODES

Hideaki Okazaki* Hideo Nakano** Takehiko Kawase***

*Gifu National College of Technology, Motosu-gun, 501-0495 Japan, okazaki@gifu-nct.ac.jp

**Shonan Institute of Technology, Fujisawa-shi, 251-0046 Japan, nakanoh@mech.shonan-it.ac.jp

*** Waseda University, Tokyo, 169-0072 Japan, kawase@mn.waseda.ac.jp

ABSTRACT

A circuit realization of an autonomous flip-flop circuit used by piecewise linear tunnel diodes, producing chaotic and bifurcation behavior, are proposed. The proposed circuit is made of four linear passive element (2 capacitors, 1 inductor, 1 resistor), one active element (1 DC battery) and two piecewise linear characteristic nonlinear resistors realized by using an operational amplifier. Typical global behavior in the circuit are illustrated. By using an analysis of the one-dimensional Poincaré map constructed from experimental data, chaotic behavior are examined, and the Liapunov exponents are estimated. The experimental observations are compared with the digital computer simulations.

1. INTRODUCTION

The present authors reported elsewhere[1]-[7], the dynamics of a third-order autonomous system representing a flip-flop circuit used by two tunnel diodes that is first studied by Moser[8]. In case that the system has the combination of saddle-spiral-2 and repeller spiral-3 type equilibrium points (i.e., the saddle repeller spiral connection), they first found out the following manifold global behavior in the system by computer simulations: (1) chaotic behavior, (2) bifurcation processes from periodic states to chaotic states in the case of varying system parameters, (3) coexistence of many periodic or chaotic attractors, and unstable saddle type closed orbits between attractors.

Further in order to clarify the detailed global behavior of the system, in particular, bifurcation processes of periodic orbits, generation of chaotic states, and manifold bifurcation processes in the unstable system parameter region where periodic or chaotic attractors exist, they made some piecewise linear approximations of the tunnel diodes characteristic of the system. Then they proposed the piecewise linear (PWL) model that has the global behavior resembling those of the original system mentioned before, and precisely investigated some of rich manifold behavior of the PWL model.

Until now, some autonomous electrical circuits exhibiting chaotic behavior have been proposed and investigated[9]-[14]. The notable autonomous electrical circuits exhibiting chaotic behavior studied by many researchers (e.g., Chua's circuit, or the circuit proposed by Shinriki et al. e.t.c), have the so-called saddle connection of equilibrium points. The chaotic behavior in nonlinear circuits having the other connections, e.g., the saddle-repeller spiral connection of equilibrium points has been seldom studied. In addition to this, it is well known that some electrical circuits with many nonlinear elements, in series or parallel, are often described by coupled Lié nard equations (a kind of Bonhoeffer van der Pol equations). It is also understood that the detail investigations of their coupled equations are important. Since the system mentioned before has the saddle-repeller spiral connection and is regarded as the typical example of coupled Lié nard equations having a symmetrical form, it is meaningful to provide a circuit realization for demonstrating global behavior including chaos and bifurcation processes of the system for demonstrations, research, and educational purposes. The purpose of this paper is to propose a circuit realization of the third-order autonomous system studied by the authors, and to report experimental results showing that chaotic behavior and bifurcation processes can occur in the proposed circuit.

2. A THIRD-ORDER AUTONOMOUS FLIP-FLOP CIRCUIT

2.1 Dynamics

Consider the circuit shown in Fig.1 and the piecewise linear v-i characteristic of the modeled tunnel diode (i.e. nonlinear resistor) shown in Fig.2. The state equations for the circuit is described by

$$C_1\frac{dv_{c1}}{dt} = i_L - f(v_{c1})$$

$$C_2\frac{dv_{c2}}{dt} = -i_L - f(v_{c2})$$

$$L\frac{di_L}{dt} = E - R\,i_L - v_{c1} + v_{c2} \qquad (1)$$

where f(•) is a piecewise linear function defined by

$$f(v_{NR}) = 2G_0 \cdot v_{NR} - \frac{6}{10}G_0 \cdot \{|v_{NR} - B_{pd}| - |v_{NR} + B_{pd}|\} + \frac{11}{10}G_0\{|v_{NR} - Bp| - |v_{NR} + Bp|\}. \qquad (2)$$

The modeled tunnel diode is given as a nonlinear resistor (NR) which is odd-symmetric characteristic shown in Fig. 2.; G_0, $G_1 = -G_0/5$, and $G_2 = 2G_0$ are the slopes in the sectionwise linear region; ±Bpd, and ±Bp denote the break points.

0-7803-4455-3/98/$10.00 © 1998 IEEE

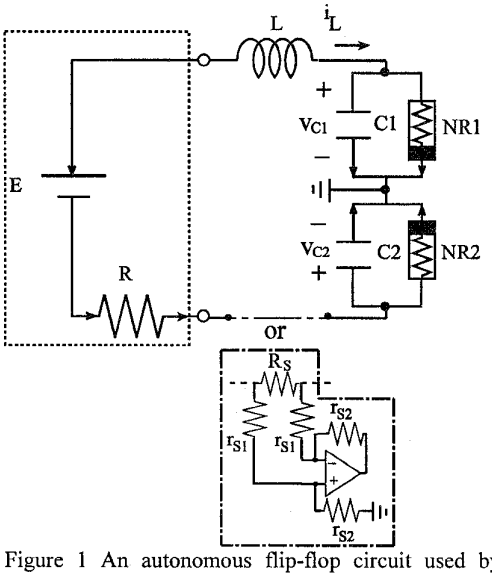

Figure 1 An autonomous flip-flop circuit used by piecewise linear tunnel diodes

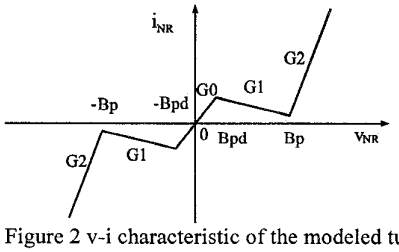

Figure 2 v-i characteristic of the modeled tunnel diode

The state equations (1) are transformed into the following non-dimensional equations :

$$\frac{dv_k}{d\tau} = B_k (i - F(v_k)), k = 1, 2,$$

$$\frac{di}{d\tau} = \frac{1}{B_1 + B_2} (E^* - R^* i - v_1 - v_2), \qquad (3)$$

where $F(v_k) = f(V_{max}\, v_k)/ I_{max}$ (k =1,2), $v_1 = v_{c1}$ /Vmax, $v_2 = -v_{c2}/V_{max}$, $i = i_L / I_{max}$, $R^* = R/R_{max}$, $E^* = E/v_{max}$, $B_k = 1/(R_{max}\, \omega\, C_k)$, k=1, 2, $\tau = \omega t$, $\omega = \sqrt{(1/C_1 + 1/C_2)}\, 1/L$, $R_{max} = V_{max} / I_{max}$, V_{max} : representative voltage value , I_{max} : representative current value. When the parameters B_1 and B_2 are identical, the equations (3) are in the mirror symmetry with regard to the plane $v_1 = v_2$. Equations(3) are a kind of coupled Lié nard equations having a symmetrical form.

2.2 Equilibrium points

The equilibrium points in eqs.(3) are determined by

$$i - F(v_k) = 0, k = 1, 2, \qquad (4)$$

$$E^* - R^* i - v_1 - v_2 = 0. \qquad (5)$$

The equation (4) represents the composed characteristic of two NR' s shown as Fig. 3. The composed characteristic (4) is not only in the mirror symmetry with the regard to the plane $v_1 = v_2$, but also is symmetry with respect to the origin, i.e. that is invariant under the transformation $(v_1, v_2, i) \rightarrow (-v_1, -v_2, -i)$. Figure 3 illustrates the composed characteristic in the region D^+ : $\{(v_1, v_2, i) \mid v_1 \geq 0, v_2 \geq 0\}$.

The non-dimensional bias battery E* and resistor R* are normally positive values. The equilibrium points are the intersection points of the composed characteristic (4) and the plane (5). Therefore, the equilibrium points exist in the region D^+. Because of the symmetry of the composed characteristic, depending on the battery polarity of E*, the equilibrium points exist in either domain D^+ or D^- : $\{(v_1, v_2, i) \mid v_1 < 0, v_2 < 0\}$. Moreover, since all the solutions are dissipative[2],[7], and the manifold global behavior mentioned before such as chaotic behavior, bifurcation processes , and the coexistence of many periodic or chaotic attractors are normally observed around unstable equilibrium points in either domain D^+ or D^- as shown in [1]-[5], [7], such behavior are not caused by six segment v-i characteristic of the NR, but are really caused by three segment v-i characteristic of it in either domain D^+ or D^-. Further unstable equilibrium points exist not on the positive resistant parts of the composed characteristic (4) (broken line segments in Fig. 3) but on that negative resistant parts (solid line segments in Fig. 3). Thus, it is sufficient to pay our attention to the region D^+, especially, to that negative resistant parts. Since the composed characteristic (4) is in the mirror symmetry, in the following sections, we focus upon the below domain including A, B, and C in Fig.3.

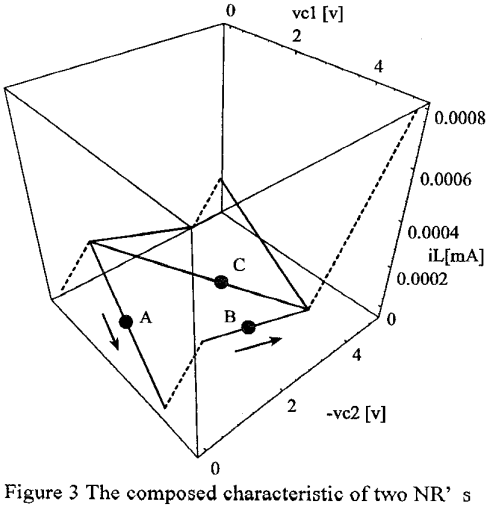

Figure 3 The composed characteristic of two NR' s

2.3 Typical Examples of Chaotic behavior observed by computer simulations

Under the conditions as follows : $G_0 = 1/2400$ [1/Ω], Bpd = 0.6 [v], Bp = 4[v], $V_{max} = 10$[v], $I_{max} = 0.5$[mA], by using fourth-order Runge-Kuttta numerical integration method with time step size equal to 0.05, the typical examples of chaotic behavior around A and B in Fig. 3 are illustrated in Fig. 4 and 5.

- In case of Fig. 4, three equilibrium points exist : $(v_1, v_2, i)_1 \approx (0.24, 0.024, 0.2)$; Eigenvalues $\sigma_1 \approx -2.59$, $\alpha_1 \pm j\beta_1 \approx 0.014 \pm j0.49$, $(v_1, v_2, i)_2 \approx (0.024, 0.24, 0.2)$; Eigenvalues $\sigma_2 \approx -2.59$, $\alpha_2 \pm j\beta_2 \approx 0.014 \pm j0.49$, $(v_1, v_2, i)_3 \approx (0.24, 0.24, 0.2)$; Eigenvalues $\sigma_3 \approx 0.56$, $\alpha_3 \pm j\beta_3 \approx 0.12 \pm j0.9$, Liapunov exponents $(\lambda_1, \lambda_2, \lambda_3) \approx (0.035, 0.00, -2.44)$, and Liapunov dimension $L_d \approx 2.014$.
- In case of Fig. 5, three equilibrium points exist : $(v_1, v_2, i)_1 \approx (0.42, 0.19, 0.28)$; Eigenvalues $\sigma_1 \approx -5.6$, $\alpha_1 \pm j\beta_1 \approx 0.064 \pm j0.5$, $(v_1, v_2, i)_2 \approx (0.19, 0.42, 0.28)$; Eigenvalues $\sigma_2 \approx -5.6$, $\alpha_2 \pm j\beta_2 \approx 0.064 \pm j0.5$, $(v_1, v_2, i)_3 \approx (0.19, 0.19, 0.28)$; Eigenvalues $\sigma_3 \approx 0.57$, $\alpha_3 \pm j\beta_3 \approx 0.11 \pm j0.89$, Liapunov exponents $(\lambda_1, \lambda_2, \lambda_3) \approx (0.029, 0.00, -4.58)$, and Liapunov dimension $L_d \approx 2.006$.

By using the algorithm in [10], the above exponents are calculated under the condition : $\Delta\tau = 20$ with a Runge-Kutta step size equal to 0.05. Both chaotic behavior are occurred in the saddle repeller spiral connection of equilibrium points.

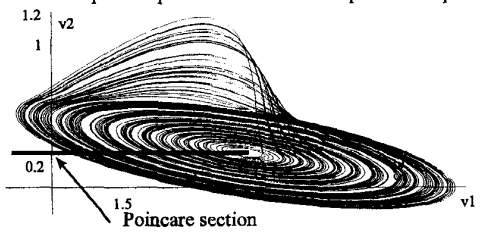

Figure 4(a) Projection onto $v_1 - v_2$ plane
($B_1 = B_2 = 0.335$, $E^* = 0.3072$, $R^* = 0.21681375$)

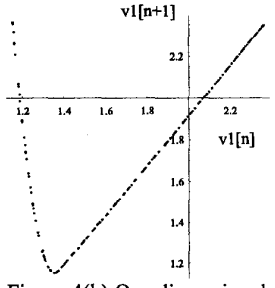

Figure 4(b) One dimensional map of v_1
(Poincaré section : $v_2 = 0.023$)

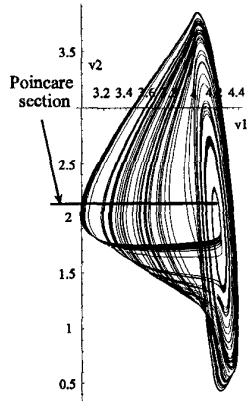

Figure 5(a) Projection onto $v_1 - v_2$ plane
($B_1 = B_2 \approx 0.34$, $E^* = 0.6772$, $R^* = 0.2348081$)

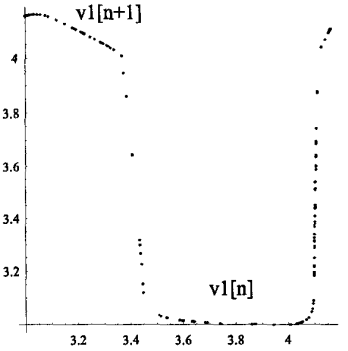

Figure 5(b) One dimensional map of v_1
(Poincaré section : $v_2 = 0.213$)

3. REALIZATION OF THE FLIP-FLOP CIRCUIT

3.1 Nonlinear Resistor

The op amp circuit used to realize the NR in Fig.1 is shown in Fig.6. The slopes and break points of the v-i characteristic in Fig.2 are given as follows:

$G_0 = 1/R_0$, $G_1 = 1/R_0 - R_1/(R_2 R_3)$, $G_2 = 1/R_0 + 1/R_1$,

$\pm Bp = Es^{\pm} R3/(R2+R3)$. Bpd: the forward voltage drop of the switching diode, Es^+ (>0) : positive saturation of the op amp, Es^- (<0): negative saturation of the op amp.

In the above, we assume that |Bp| is greater than Bpd.

Under the conditions such that $R_0 = R_1 = R_2$, and $R_3 = 10\ R_0 /12$, we have the same values of the slopes as eq.(2):

$G_0 = 1/R_0$, $G_1 = -1/5R_0$, $G_2 = 2/R_0$.

In these conditions, $\pm Bp = 10\ Es^{\pm}/22$ hold.

Since the negative resistance of the NR realized by the op amp circuit of Fig.6 is given by the op amp based negative resistance converter, the ground position of the NR is fixed. Therefore the series connection of two NR' s in the flip-flop circuit of Fig.1 brings about the ground position problem of the circuit. In order to solve the problem, as shown in Fig.1, we connect the common point of the power supplies (or batteries) Vcc^+ and Vcc^- of the op amps with the common point at which two NR's in the flip-flop circuit are connected in series.

Since Es^+ and Es^- are generally in proportion to Vcc^+ and Vcc^- respectively, for any op amps, there exist the values of Vcc^+ and Vcc^- such that $|Es^+| = |Es^-|$. Moreover, since $v_{c1} \geq 0$ and $v_{c2} \leq 0$ in D^+, for any couple of the op amp based nonlinear resistors NR1 and NR2, we can independently set up the break points such that $|Es^+_1| = |Es^-_2|$ as shown in Fig. 9, and 10, where Es^+_1 and Es^-_2 are positive and negative saturations of the op amps in NR1 and NR2, respectively. It is needless to say that Es^+_1 and Es^-_2 are independently and freely set up by Vcc^+ and Vcc^- . Further in order to avoid the dependency of the battery polarity of E in the flip-flop circuit of Fig.1, using switching diode limiters as shown in Fig.6, we make the NR has the odd-symmetric characteristic as shown in Fig.2. However, as mentioned in the preceding section, because of its odd-symmetric characteristic, the global behavior are not caused by six segment v-i characteristic of the NR, but are really caused by three segment v-i characteristic of it in either domain D^+ or D^-.

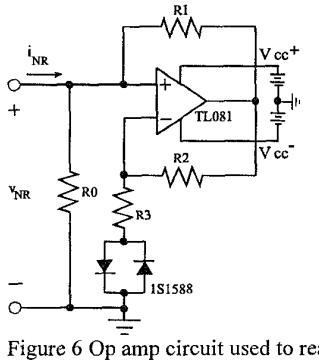

Figure 6 Op amp circuit used to realize the NR

3.2 Bias voltage source subcircuit

Since chaotic behavior and bifurcation processes are very sensitive, if the bias constant voltage source E in Fig.1 is given by a voltage supply such as series regulator, we can not neglect the power supply switching influences. Therefore we have to use a normal battery or a rechargeable battery as the constant voltage source E. In order to freely set values of E and R in the subcircuit enclosed by the broken line box in Fig.1 by using a battery with internal resistance, we construct the subcircuit in the broken line box as the circuit in Fig.7. The characteristic of the circuit in Fig.7 is given as follows:

$$E = \frac{Eb\,(1-\alpha)\,r0}{r+r0}\,, \tag{6}$$

$$R = r3 + \frac{(1-\alpha)\cdot r0\cdot(r+\alpha\,r0)}{r+r0}\,, \tag{7}$$

$$r1 = \alpha\,r0\,,\ r2 = (1-\alpha)\,r0\,,\ 0 \le \alpha \le 1\,, \tag{8}$$

where Eb: battery, r: battery internal resistance, r0: resistor, r1, r2, and r3: variable resistors.

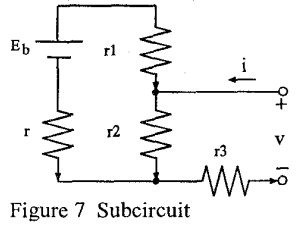

Figure 7 Subcircuit

3.3 Realization of the circuit

In this paper, the experimental results are measured and converted to digitized data by Tektronix digital real-time oscilloscope TDS340P (500MS/s), and are illustrated by using Mathematica, and FreeHand softwares. The current i_L is measured by the current monitor in the dot-dashed line box in Fig.1. Current i_L flowing in Rs resistor causes a voltage Rs i_L to appear across the resistor. An appropriate choice of Rs, r_{s1}, and r_{s2} in the monitor are 100[Ω], 10[kΩ], and 100[kΩ], respectively. As regards experiments of the actual circuit, we plot 10 Rs i_L instead of i_L.

Under the electric component values as follows:

Bpd = 0.6[V] (the forward voltage drop of 1S1588), Bp = 4[V], E_b : 13[V]; r = 1[Ω] (12v7Ah rechargeable lead acid battery), L=150[mH], C_1=1000[pF], C_2=1000[pF],r_0 = 200[Ω], r_3: 0 ~ 10[kΩ], $R_0 = R_1 = R_2$ = 2.4[kΩ] (Tolerance ± 0.1%), R_3 = 2[kΩ] (Tolerance ± 0.1%), Chaotic and bifurcation behavior can be observed in the domain D^+ by setting values of E and R appropriately (See Fig.11). Under the above component values, the v-i characteristic of the realized NR obtained by SPICE simulation, and its measured v-i characteristic, and its measured composed characteristic are shown in Fig.8, 9, and 10, respectively. The right and left in Fig. 9 illustrate the v-i characteristic of NR1 and NR2, respectively. Because of using the switching diode limiters, there exists some difference between the realized characteristic of NR and one described by eq.(2). However, the measured composed characteristic is confirmed to be in the mirror symmetry with regard to the plane v_{c1}-(-v_{c2}) in D^+.

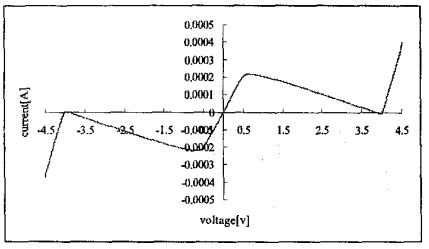

Figure 8 v-i characteristic of NR by SPICE

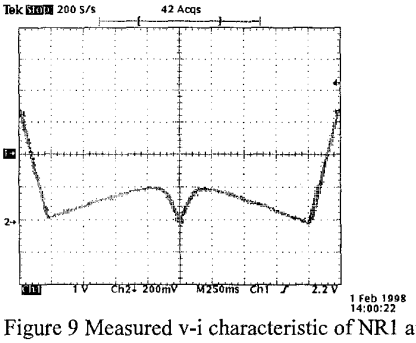

Figure 9 Measured v-i characteristic of NR1 and NR2
(Horizontal Scale 1V/div; Vertical Scale 200mV/div)

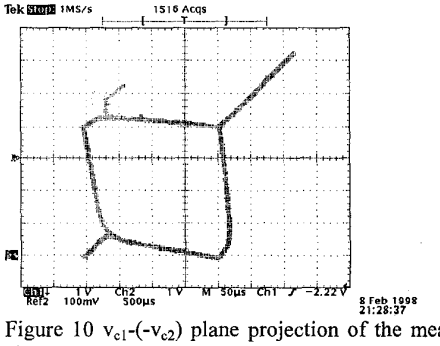

Figure 10 v_{c1}-(-v_{c2}) plane projection of the measured composed characteristic of NR1 and NR2
(Horizontal Scale 1V/div; Vertical Scale 1V/div)

4. EXPERIMENTAL RESULTS AND DISCUSSIONS

4.1 Bifurcation behavior and coexistence of attractors

We illustrate the typical behavior of the circuit in Fig. 11. The followings are the rough sketch of the results. Around A in Fig. 3, after a Hopf bifurcation, periodic attractor with period one appears. As R decrease, various bifurcation behavior are observed as shown in Fig. 11 (1)-(5). In the similar way, around B in Fig.3, as R decrease, various bifurcation behavior are also observed as shown in Fig.11(7)-(11). While bifurcation behavior around A or B occur, there always exists single periodic attractor with period one around C, as shown in Fig.11(6). Since C_1 and C_2 are identical in these experiments, this circuit vector field is in the mirror symmetry with regard to the plane v_{c1}-(-v_{c2}). It is needless to say that bifurcation behavior also occur around the mirror symmetry parts of A and B in Fig.3.

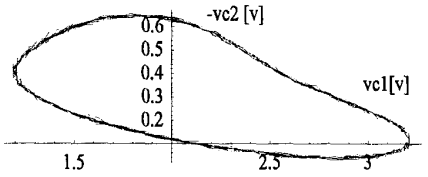

Figure 11(1) E = 3.07[v], R = 4836.116[Ω]

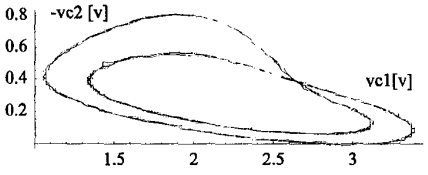

Figure 11(2) E = 3.07, R = 4654.116[Ω]

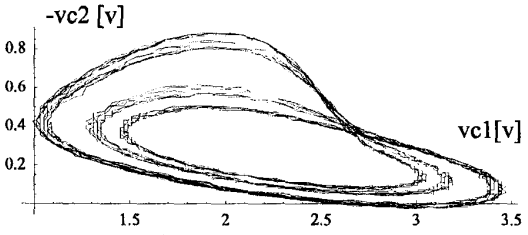

Figure 11(3) E = 3.07[v], R = 4564.116[Ω]

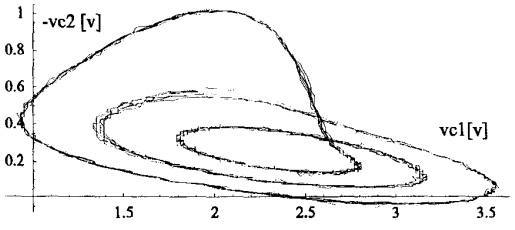

Figure 11(4) E = 3.07[v], R =4426.116[Ω]

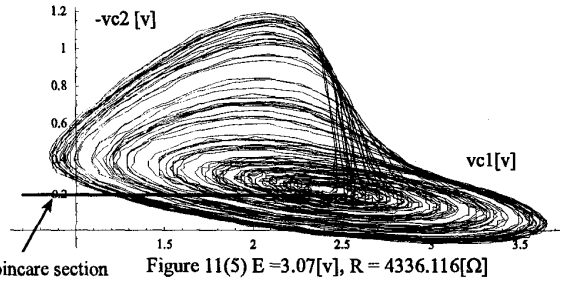

Figure 11(5) E =3.07[v], R = 4336.116[Ω]

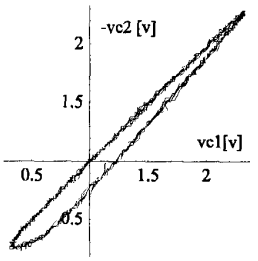

Figure 11(6) E=3.07[v], R = 3236.116[Ω]

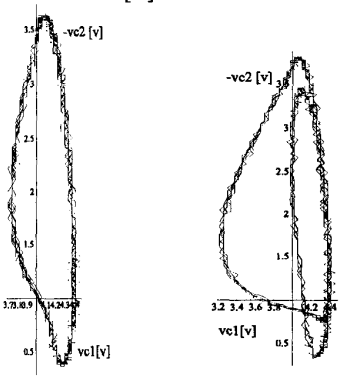

Figure 11(7) E = 6.772[v], R = 4970.116[Ω]

Figure 11(8) E = 6.772[v], R = 4750.162[Ω]

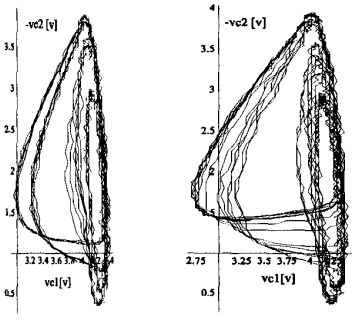

Figure 11(9) E = 6.772[v], R = 4690.162[Ω]

Figure 11(11) E = 6.772[v], R = 4628.162[Ω]

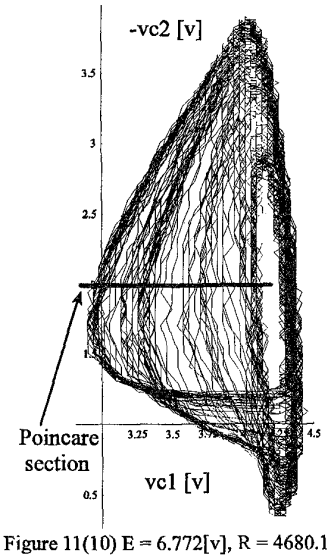

Figure 11(10) E = 6.772[v], R = 4680.162[Ω]

4.2 Chaotic behavior

Fig.11(5) and (10) illustrate the typical examples of chaotic behavior around A and B in Fig.3,respectively. In case of Fig.11(5) and (10), the derived one dimensional Poincaré map from the experimental data by using a least square method and an approximated polynomial function, and the experimental data plots are shown in Fig.12(a) and (b), respectively. Power spectrum in case of Fig.11(5) and (10), are also illustrated in Fig.13(a) and (b), respectively. Further the projections onto v_{c1}-i_L, and $(-v_{c2})$-i_L planes of the chaotic behavior in case of Fig.11(5), are illustrated in Fig.14(a), and (b).

- In case of Fig. 11(5), Liapunov exponent $\lambda_1 \approx 0.62$.
- In case of Fig. 11(10), Liapunov exponent $\lambda_1 \approx 0.37$.

By using the derived one dimensional maps, the above exponents are estimated.

The above chaotic behavior of the actual circuit and those of the state equations(3) in Fig.4, and 5 closely resemble each other.

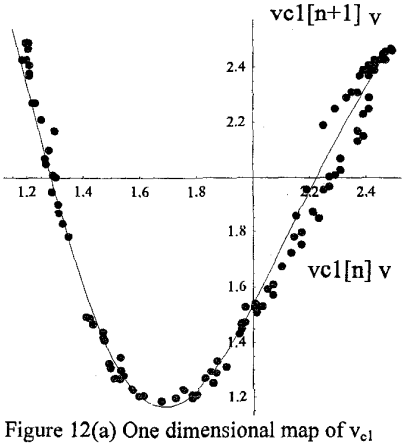

Figure 12(a) One dimensional map of v_{c1}
(Poincaré section : $v_{c2} = 0.2$)

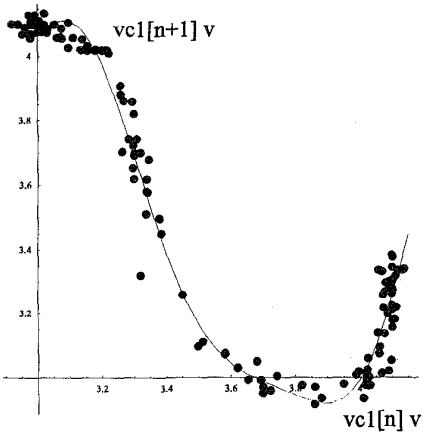

Figure 12(b) One dimensional map of v_{c1}
(Poincaré section : $v_{c2} = 2.0$)

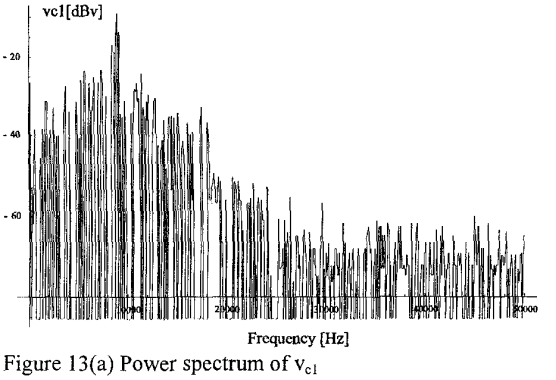

Figure 13(a) Power spectrum of v_{c1}

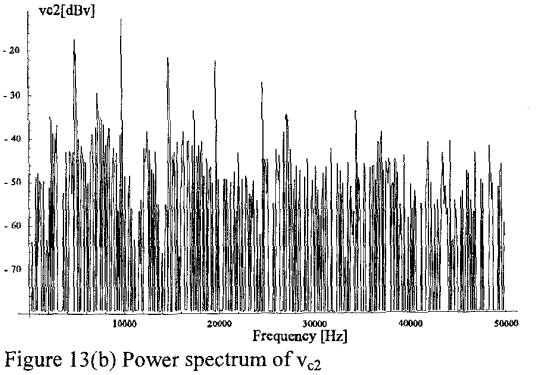

Figure 13(b) Power spectrum of v_{c2}

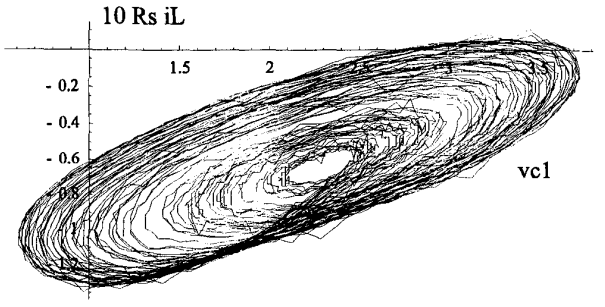

Figure 14(a) Projection onto v_{c1}-i_L plane

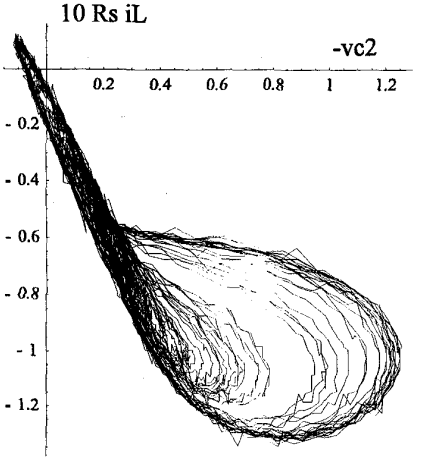

Figure 14(a) Projection onto $(-v_{c2})$-i_L plane

5. CONCLUSIONS

The following results are obtained:
(1) Chaotic behavior and bifurcation processes really appear in the actual flip-flop circuit used by three-segment piecewise linear resistors.
(2)Experimental observations, for example, chaotic behavior and bifurcation processes, and digital computer simulations closely resemble each other.
(3)For typical chaotic behavior observed in the circuit dynamics, sets of one positive, one nearly zero and one negative Liapuov exponents are found by digital computations.

ACKNOWLEDGEMENT

The authors are grateful to the students of Gifu National College of Technology: Mr. Takayuki Hirose, Mr. Takashi Hirata, Mr. Shinji, Takasaki, and Mr. Kazuaki Sugio for their help in the experiments and the simulations.

REFERENCES

[1] H.Okazaki, M. Yamazaki, H. Nakano, and T. Kawase," Non-periodic Behavior Observed in a Parallel Blower System",SICE1987,ES1-5, Hiroshima, July, pp. 977- 980, 1987.

[2] H. Okazaki, H. Nakano, and T. Kawase, " The Parameter Space of a Parallel Blower System",(Aoki ed.) Dynamical Systems and Applications, Vol. 5, pp. 183-203, World Scientific, 1987.

[3] H.Okazaki, M. Inoue, T. Sakurai, H. Nakano, and T. Kawase, "Piecewise-Linear Modelling and Analysis on Nonlinear Behavior in a Parallel Blower System Model - Analysis Using Global One Dimensional Mapping Method-", 11th U.S.National Congress of Applied Mechanics, Tucson, Arizona,1990.

[4] H. Okazaki, U. Uwaba, H. Nakano, and T. Kawase, " Bifurcation Set of a Modelled Parallel Blower System", IEICE Transactions on Fundamentals of Electronics, Communications and Computer Sciences, Vol. E76-A, No.3, pp. 299- 309, 1993.

[5] H. Okazaki, H. Nakano, and T. Kawase, " Global Dynamic Behaviour of a Parallel Blower System", IEICE Transactions on Fundamentals of Electronics, Communications and Computer Sciences, Vol. E78-A, No.6, pp. 715- 726, 1995.

[6] H. Okazaki, K. Hayakawa, A. Tanaka, and H. Nakano, " Coupled Flip-Flop Circuits Producing Chaotic States - Application to Secure Communication- ", Proc. of NOLTA 95 1E-2, pp. 137-140, 1995.

[7] H. Okazaki, "A Study of Nonlinear Dynamic Phenomena Observed in a Third Order Autonomous System", Doctoral Thesis, Waseda University, Tokyo, Japan, 1996.

[8] J.K. Moser, "Bistable Systems of Differential Equations with Applications to Tunnel Diode Circuits," IBM J. Res. Dev. 5, pp.226-240, 1961.

[9] M. Shinriki, M. Yamamoto, and S. Mori, "Multimode oscillations in a modified van der Pol oscillator containing a positive nonlinear conductance", Proc. of IEEE, Vol. 69, pp. 394-395, Mar, 1981.

[10] T. Matsumoto, L. O. Chua, and M. Komuro, " The Double Scroll" , IEEE Trans. Circuits Syst., Vol. CAS-32, pp. 798-818, 1985.

[11] G-Q. Zhong and F. Ayrom, "Experimental confirmation of chaos from Chua's circuit" , Int. J. Circuit Theory Appl., Jan. 1985.

[12] E. Freire, L. G. Franguelo, and J. Aracil, "Periodicity and chaos in an autonomous electronic system", IEEE Trans. Circuits Syst., Vol. CAS-31, pp. 237-247, Mar. 1984.

[13] T. Matsumoto, L.O. Chua and K. Tokumatsu, "Double Scroll via a Two-Transistor Circuit", IEEE Trans. Circuits Syst., Vol. CAS-33, pp. 828-835, Aug. 1986.

[14] M. T. Abuelma' atti and M. K. Aiyad, "Chaos in Autonomous Active-R Circuit", IEEE Trans. Circuits Syst., Vol. CAS-42, pp. 1-5, Jan. 1995.